

Effective Range Analysis of s -Wave K^-p Reactions

GORDON L. SHAW*

University of California, San Diego, La Jolla, California

AND

MARC H. ROSS†

Indiana University, Bloomington, Indiana

(Received October 25, 1961)

An effective range analysis of s -wave K^-p reaction data is carried out. Two specific problems are investigated. First, a survey is made of solutions which, in addition to fitting the above threshold data, yield a $\pi\Lambda$ resonance having the characteristics of the Y_1^* . The only acceptable solutions found were for even $K\Sigma N$ parity and did not lead to a Y_0^* resonance. Other features of these solutions are discussed, as well as the validity and applicability of the effective range approximation to describe the energy dependence of the $\bar{K}N$ data. Second, using the (nonperturbative) uncoupled phase procedure developed in the preceding paper, we investigate effective range solutions for the above threshold K^-p data which, in the absence of influence of the $\bar{K}N$ channel, would have the pion-hyperon scattering amplitudes predicted by global

symmetry of the pion-baryon interaction. The concept of global symmetry is found to be compatible with the present K^-p data. The actual πY phases, however, are quite different from the global symmetry uncoupled phases in states coupled to the $\bar{K}N$ s wave, and there are solutions in which the Y_0^* arises as a quasi-bound state resonance. Going beyond the physical predictions of these surveys, we conclude that there are at present almost enough $\bar{K}N$ data above threshold to justify a search for effective range solutions (then predicting whether either Y_1^* or Y_0^* is in the same partial wave as a $\bar{K}N$ s state). Moreover, it is clear that such solutions will be quite different from the results of a constant scattering-length analysis of low-energy data.

I. INTRODUCTION

WE perform a phenomenological analysis of s -wave K^-p data using the formalism presented in the preceding paper.¹ The energy dependence of the scattering amplitudes are parametrized by the effective range approximation (the effects of the K^-p – \bar{K}^0n mass difference and the charged K^-p channel are taken into account).

We find that the present data do not warrant a full search for effective range solutions of the above threshold data. Thus we principally investigate certain types of solutions. The feasibility of performing a full search for solutions in the near future is studied in Sec. V.

There are two separate purposes in this work: (1) to investigate from a purely phenomenological analysis the consequences of the proposal that the Y_1^* , the $\Lambda\pi$ resonance located at ≈ 50 Mev below the K^-p threshold, is associated with the s -wave $\bar{K}N$ system and may perhaps be describable as a quasi-bound state of that system²; (2) to investigate the compatibility of the

concept of global symmetry of the pion-baryon interaction with the s -wave K^-p data.

The three-body channels ($Y+2\pi$) which are coupled to the s -wave $\bar{K}N$ system are known to have quite small production cross section in the energy region of our analysis (incident K^- laboratory momentum ≤ 400 Mev/c). Thus we can hope that we only need consider the coupled two-body channels and can apply the multichannel effective range formalism of Sec. II of I to describe the energy dependence of the isotopic spin $I=0$ and 1 s -wave $\bar{K}N$ systems. The validity of the effective range approximation for the present problem will be discussed in Sec. V. The additional energy dependences induced by isotopic spin violating virtual electromagnetic interactions are treated using the formalism of Sec. III of I.

To describe all possible reactions, at a particular energy, among the coupled channels of the s -wave $\bar{K}N$ system, nine "zero-range" parameters are needed: six for the $I=1$ system of $\bar{K}N$, $\Sigma\pi$, $\Lambda\pi$ and three for the $I=0$ system of $\bar{K}N$, $\Sigma\pi$. In order to use the full effective range formalism to analyze the s -wave K^-p data all nine zero-range parameters are needed in addition to ranges which can be roughly estimated *a priori*. Starting from a $\bar{K}N$ initial state there are only six possible measurements at a given energy. In the presence of extensive and accurate data involving the K^-p channel we could use the energy dependence specified by the effective range formalism to determine all the parameters. This possibility does not seem unlikely since several of the cross sections may display considerable energy dependence (for example, the elastic K^-p cross section does drop off very rapidly).

association of the Y_1^* with the $\bar{K}N$ s state, we survey solutions which tend to correspond to the quasi bound state picture and that the example shown, Fig. 1, is of this type.

* Supported in part by the U. S. Atomic Energy Commission.

† Supported in part by the National Science Foundation.

¹ G. Shaw and M. Ross, Phys. Rev. **126**, 806 (1962), preceding paper. We shall refer to this paper as I.

² There are two natural mechanisms which give rise to resonances in elementary reactions: A metastable system can be a bound state associated with closed channels which is weakly coupled to the open channels or it may arise essentially through the open channels by an attractive interaction within the angular momentum barrier. In either case the resonance can be described by the multichannel effective range formula (but not necessarily in the scattering-length approximation), but its characteristics are quite different: the width will be smaller in the quasi-bound-state case and there is considerable difference in shape between the two. With present information we cannot attempt to distinguish the resonances from these characteristics; however, one can examine the details of effective range solution in the closed and in the open channels and judge if they correspond roughly to the bound-state condition or to an angular momentum resonance, respectively. The reader can observe in Sec. III that, in our investigation of the

However, at present, we cannot expect to determine all these parameters solely from the known energy dependences of the above threshold K^-p data. Thus, we are led to discuss the two situations mentioned above in which we assume additional information about the physical situation and reach useful conclusions.

A $\Lambda\pi$ resonance Y_1^* at 1385 Mev total energy has recently been observed by several experimental groups.³ One of the proposed theoretical explanations of the Y_1^* is that it is a quasi-bound state of the s wave, $I=1$ $\bar{K}N$ channel. In fact, Dalitz and Tuan,⁴ from their constant-scattering-length analysis of the rough s -wave K^-p data predicted that such a resonant state might exist. Discovery of the Y_1^* led Ross and Shaw⁵ to discuss the possibility of putting the association of the Y_1^* with the $\bar{K}N$ s state to a detailed test by means of an effective range analysis, and as a result determine the KYN parities P .

The angular distribution of the $\Lambda\pi$ indicates that the spin of the Y_1^* is likely to be $J=\frac{1}{2}$, whereas its parity is not known. We will assume that the Y_1^* has $J=\frac{1}{2}$ and $P(KY_1^*N)$ is even, i.e., the $\Lambda\pi$ resonance is associated with the s -wave $\bar{K}N$ system. Thus any effective range solutions for the s -wave $\bar{K}N$ system must fit the resonance parameters of the Y_1^* . The details of an extensive survey of solutions are given in Sec. III.⁶ We will see that with our assumption we are led to some significant conclusions, the most important being that the only acceptable solutions found were for the channel in a p state, thus there is even $K\Sigma N$ parity. In addition, this analysis of the above threshold data suggests that both the Y_1^* and Y_0^* , the $I=0$ $\Sigma\pi$ resonance at ≈ 1405 Mev,⁷ should not be associated with the $\bar{K}N$ s state.

The second problem we investigate involves abandoning the purely phenomenological approach. We instead test theories which make definite predictions about the pion-hyperon phases $\phi_{\pi Y}$. These theories actually predict "uncoupled" πY amplitudes $\phi_{\pi Y}$ which describe an idealized πY system in the absence of coupling to the $\bar{K}N$ channel. We have attempted to develop a workable and meaningful theory which enables us to confront the $\phi_{\pi Y}$ with experiment. A nonperturbative approximation (the uncoupled-phase method) for calculating the actual πY amplitudes from the $\phi_{\pi Y}$ and the (measured) scattering length in the $\bar{K}N$ channel plus production ratios from the $\bar{K}N$ channel to the πY channels is given

in Sec. IV of I. The uncoupled phase method allows for conditions in which the actual scattering amplitudes among the πY channels are *strongly* influenced by the coupling to the $\bar{K}N$ channel.

The specific theoretical model we consider in Sec. IV is global symmetry of the pion-baryon interactions.⁸ Since we consider only the partial wave corresponding to $J=\frac{1}{2}$, we are investigating the consequences of weak "uncoupled" πY scattering. The uncoupled-phase method together with the assumption of global symmetry is used to help determine the "zero-range" $\bar{K}N$ parameters; the number of free parameters is thus decreased by four. An effective range analysis of the above threshold s -wave K^-p data is carried out. The results indicate that the concept of global symmetry is compatible with the present data. The actual $\phi_{\pi Y}$, in the *partial wave considered*, are found to be greatly modified from the global symmetry $\phi_{\pi Y}$. (Previous, less elaborate, calculations⁹ done at specific energies—not employing the effective range formalism—led to the same general conclusions.)

Solutions with global symmetry $\phi_{\pi Y}$ were found which fit the Y_0^* . The great importance of this lies in the fact that all three observed pion-hyperon resonances can thus be explained by one attractively simple description. The explanation of the Y_1^* (as opposed to the quasi bound state picture) is that it is a consequence of the attractive p -wave πY scattering in global symmetry which, in analogy with the $J=\frac{3}{2}$, $I=\frac{3}{2}$ pion-nucleon resonance, yields a $J=\frac{3}{2}$, $I=1$ resonance having a position, width and Σ/Λ branching ratio fairly close to that observed for the Y_1^* . It also predicts another $J=\frac{3}{2}$, $I=2$ resonance at ~ 1540 Mev (i.e., the position of the $Y_1^*+2m_\Sigma-2m_\Lambda$). Preliminary results of a counter experiment at CERN¹⁰ analyzing the K^+ produced in π^- collisions with protons show a third πY resonance, " Y_e^* ," at ~ 1580 . This, of course, lends strong support to the global-symmetry model of the pion-hyperon interactions. (Runs are planned with deuterium targets to determine whether the Y_e^* has $I=1$ or 2 .) Thus the Y_1^* and Y_e^* are possibly global symmetry resonances and the Y_0^* a quasi-bound state of the s -wave $\bar{K}N$ system.

II. ENERGY DEPENDENCE OF s -WAVE K^-p CROSS SECTIONS

In this section we will display the explicit energy dependence of the s -wave K^-p cross sections in the effective range approximation. We will label the channels for a given isotopic spin by the strangeness-carrying particle: $\bar{K}\equiv\bar{K}N$, $\Sigma\equiv\Sigma\pi$, $\Lambda\equiv\Lambda\pi$; when we are referring to channels coupled to the K^-p initial state, the label will also carry the charge of the strange-

³ M. Alston, L. Alvarez, P. Eberhard, M. Good, W. Graziano, H. Ticho, and S. Wojcicki, Phys. Rev. Letters **5**, 520 (1960). J. Berge, P. Bastien, O. Dahl, M. Ferro-Luzzi, J. Kirz, D. Miller, J. Murray, A. Rosenfeld, R. Tripp, and M. Watson, *ibid.* **6**, 557 (1961). H. Martin, L. Leipuner, W. Chinowsky, F. Shively, and R. Adair, *ibid.* **6**, 283 (1961).

⁴ R. Dalitz and S. Tuan, Phys. Rev. Letters **2**, 425 (1959); Ann. Phys. **10**, 307 (1960).

⁵ M. Ross and G. Shaw, Phys. Rev. Letters **5**, 578 (1960). See also R. H. Dalitz, *ibid.* **6**, 239 (1961).

⁶ G. Shaw and M. Ross, Phys. Rev. Letters **7**, 210 (1961). The results of the survey have been reported in this paper.

⁷ M. Alston, L. Alvarez, P. Eberhard, M. Good, W. Graziano, H. Ticho, and S. Wojcicki, Phys. Rev. Letters **6**, 698 (1961).

⁸ M. Gell-Mann, Phys. Rev. **106**, 1296 (1957).

⁹ M. Ross and G. Shaw, Phys. Rev. **115**, 1773 (1959); Bull. Am. Phys. Soc. **5**, 504 (1960).

¹⁰ A. Lundby, J. Dowell, B. Leontic, R. Meunier, J. Stroot, and M. Steptycha (private communication from B. Leontic).

ness-carrying particle, e.g., $\sigma_{K^- \bar{K}^0}$ is the cross section for the charge-exchange process $K^- + p \rightarrow \bar{K}^0 + n$.

The (3×3) $I=1$ T matrix is written as

$$T^1(E) = (k^{l+\frac{1}{2}})[M^1 - i(k^{l+\frac{1}{2}})^2]^{-1}(k^{l+\frac{1}{2}}), \quad (2.1)$$

where

$$(k^{l+\frac{1}{2}}) = \begin{bmatrix} k_{\bar{K}}^{l+\frac{1}{2}} & 0 & 0 \\ 0 & k_{\Sigma}^{l+\frac{1}{2}} & 0 \\ 0 & 0 & k_{\Lambda}^{l+\frac{1}{2}} \end{bmatrix}, \quad (2.2)$$

$$M^1 = \begin{bmatrix} M_{\bar{K}\bar{K}^1}(E) & M_{\bar{K}\Sigma^1}(E) & M_{\bar{K}\Lambda^1}(E) \\ M_{\bar{K}\Sigma^1}(E) & M_{\Sigma\Sigma^1}(E) & M_{\Sigma\Lambda^1}(E) \\ M_{\bar{K}\Lambda^1}(E) & M_{\Sigma\Lambda^1}(E) & M_{\Lambda\Lambda^1}(E) \end{bmatrix}, \quad (2.3)$$

and the M_{ij} are all real even functions of the k_i . Below the i th threshold,

$$k_i \rightarrow i\kappa_i, \quad \kappa > 0. \quad (2.4)$$

The effective range approximation (2.22) of **I** is that the nondiagonal elements are to a good approximation constant with energy,

$$M_{\bar{K}\Sigma^1}(E) = M_{\bar{K}\Sigma^1}(E_0), \quad M_{\bar{K}\Lambda^1}(E) = M_{\bar{K}\Lambda^1}(E_0), \\ M_{\Sigma\Lambda^1}(E) = M_{\Sigma\Lambda^1}(E_0), \quad (2.5)$$

whereas the diagonal elements may be written as

$$M_{\bar{K}\bar{K}^1}(E) = M_{\bar{K}\bar{K}^1}(E_0) + \frac{1}{2}R_{\bar{K}}[k_{\bar{K}}^2 - k_{\bar{K}}^2(E_0)], \quad (2.6)$$

$$M_{\Sigma\Sigma^1}(E) = M_{\Sigma\Sigma^1}(E_0) + \frac{1}{2}c_{I\Sigma}R_{\Sigma}^{-2I\Sigma+1} \\ \times [k_{\Sigma}^2 - k_{\Sigma}^2(E_0)], \quad (2.7)$$

$$M_{\Lambda\Lambda^1}(E) = M_{\Lambda\Lambda^1}(E_0) + \frac{1}{2}c_{I\Lambda}R_{\Lambda}^{-2I\Lambda+1} \\ \times [k_{\Lambda}^2 - k_{\Lambda}^2(E_0)], \quad (2.8)$$

where

$$c_{I=0} = 1 \quad \text{and} \quad c_{I=1} = -3. \quad (2.9)$$

R_i is a measure of the range of forces in channel i . We take the energy E_0 to be the K^-p threshold: 1433 Mev. For the $I=0$ T matrix we have similar relations except that all the matrices are (2×2) , there being no Λ channel.

The corrections (see Sec. III of **I**) for the $K^-p - \bar{K}^0n$ mass difference and the Coulomb field in the K^-p channel are taken into account by introducing the energy-dependent complex scattering lengths a_I ,¹¹

$$T_{\bar{K}\bar{K}}^I \equiv -a_I k_{\bar{K}}(1 + ia_I k_{\bar{K}})^{-1}, \quad (2.10)$$

and defining (with $k_{\bar{K}} = k_{K^-}$)

$$\tilde{T}_{\bar{K}i}^0 = \frac{T_{\bar{K}i}^0(1 + ia_0 k_{K^-})(1 + ia_1 k_{\bar{K}}^0)}{[1 + \frac{1}{2}i(a_0 + a_1)(\tilde{k}_{K^-} + k_{\bar{K}}^0) - a_0 a_1 \tilde{k}_{K^-} k_{\bar{K}}^0]}, \quad (2.11a)$$

$$\tilde{T}_{\bar{K}i}^1 = \frac{T_{\bar{K}i}^1(1 + ia_1 k_{K^-})(1 + ia_0 k_{\bar{K}}^0)}{[1 + \frac{1}{2}i(a_0 + a_1)(\tilde{k}_{K^-} + k_{\bar{K}}^0) - a_0 a_1 \tilde{k}_{K^-} k_{\bar{K}}^0]}, \quad (2.11b)$$

¹¹ The scattering length is defined such that $-1/a = k_{\bar{K}} \cot \delta$. Note the minus sign.

where

$$\tilde{k}_{K^-} = c^2 k_{K^-} + i2B^{-1}[\ln(2k_{K^-} R_{K^-}) \\ + k_{K^-}^{-2} B^{-2} \sum_{m=1}^{\infty} m^{-1}(m^2 + k_{K^-}^{-2} B^{-2})^{-1} + 0.577], \\ c^2 = 2\pi k_{K^-}^{-1} B^{-1}[1 - \exp(-2\pi k_{K^-}^{-1} B^{-1})]^{-1}, \quad (2.12)$$

and the Bohr radius¹² $B = 83$. Then the cross sections for the reactions with the K^-p as the initial state are

$$\frac{d\sigma_{K^- K^-}}{d\Omega} = \frac{1}{4k_{K^-}^{-2}} \left| c^2(\tilde{T}_{\bar{K}\bar{K}^1} + \tilde{T}_{\bar{K}\bar{K}^0}) \right. \\ \left. + \frac{\csc^2(\theta/2)}{k_{K^-} B} \exp\left(\frac{2i}{k_{K^-} B} \ln \sin(\theta/2)\right) \right|^2, \quad (2.13)$$

$$\sigma_{K^- \bar{K}^0} = \frac{c^2 \pi k_{\bar{K}}^0}{k_{K^-}} |\tilde{T}_{\bar{K}\bar{K}^1} - \tilde{T}_{\bar{K}\bar{K}^0}|^2, \quad (2.14)$$

$$\sigma_{K^- \Sigma^{\pm}} = \frac{2\pi c^2}{k_{K^-}^{-2}} \left| \frac{1}{\sqrt{2}} \tilde{T}_{\bar{K}\Sigma^1} \pm \frac{1}{\sqrt{3}} \tilde{T}_{\bar{K}\Sigma^0} \right|^2, \quad (2.15)$$

$$\sigma_{K^- \Sigma^0} = \frac{2\pi c^2}{3k_{K^-}^{-2}} |\tilde{T}_{\bar{K}\Sigma^0}|^2, \quad (2.16)$$

$$\sigma_{K^- \Lambda} = \frac{2\pi c^2}{k_{K^-}^{-2}} |\tilde{T}_{\bar{K}\Lambda^1}|^2. \quad (2.17)$$

The "total" elastic cross section $\sigma_{K^- K^-}$ is taken as

$$\sigma_{K^- K^-} = \frac{20}{17} \times 2\pi \int_{-1}^{0.7} d\cos\theta \frac{d\sigma_{K^- K^-}}{d\Omega}. \quad (2.18)$$

There exist three different types of experiments involving low-energy $\bar{K}N$ systems: (a) Low energy in flight K^-p reactions. These are known to be s wave (for $\bar{K}N$) for incident K^- momenta $\lesssim 225$ Mev/ c . (b) The at-rest capture of K^- from Bohr orbits of (K^-, p) atoms. Day, Snow, and Sucher¹³ have given arguments to show that the K^- is captured from high s orbitals. It has been shown¹⁴ that the experiment of Fields *et al.*¹⁵ on the absorption rate of stopped π^- in hydrogen lends added support to the Day, Snow, Sucher conclusion that capture from p states is suppressed in (K^-, p) atoms. (c) The Y^* resonance experiments. The possible connection of the Y_1^* with the $\bar{K}N s$ state will be the subject of Sec. III. We will now summarize the experimental K^-p results (a), (b) and list values of cross sections used in the effective range analysis of Secs. III and IV.

¹² Except when noted otherwise, lengths are measured in fermis ($1f = 10^{-13}$ cm) and momenta in f^{-1} .

¹³ T. Day, G. Snow, and J. Sucher, Phys. Rev. Letters **3**, 61 (1959).

¹⁴ J. Russell and G. Shaw, Phys. Rev. Letters **4**, 369 (1960).

¹⁵ T. Fields, G. Yodh, M. Derrick, and J. Fetkovich, Phys. Rev. Letters **5**, 69 (1960).

(a) The general features of the in-flight K^-p data are as follows: The threshold for $\sigma_{K^-K^0}$ occurs at a laboratory K^- momentum of 90 Mev/ c and $\sigma_{K^-K^0}$ stays quite small compared to $\sigma_{K^-K^-}$ at all energies. There is a possible rapid variation of $\sigma_{K^-K^+}/\sigma_{K^-K^-}$ with energy for momenta <125 Mev/ c ; above this momentum the ratio is roughly constant (~ 1). At 300 Mev/ c , there is definitely p wave present, and it becomes dominant at 400 Mev/ c . The 400-Mev/ c data provide a very strong restriction on the s -wave elastic scattering^{16,17}

$$\sigma_{K^-K^-}(400 \text{ Mev}/c) < 22. \quad (2.19)$$

The strong energy dependence needed to produce the falloff in from its large values at lower energies cannot be fitted in the constant scattering length approximation. In addition to (2.19) we use the 175-Mev/ c values¹⁸:

$$70 < \sigma_{K^-K^-} < 90, \quad (2.20)$$

$$11 < \sigma_{K^-K^0} < 19, \quad (2.21)$$

$$33 < \sigma_{K^-K^+} + \sigma_{K^-K^-} < 49, \quad (2.22)$$

$$0.5 < \sigma_{K^-K^+}/\sigma_{K^-K^-} < 2.0. \quad (2.23)$$

(b) The at-rest capture of K^- in hydrogen yield the hyperon ratios $\Sigma^-\pi^+/\Sigma^+\pi^-/\Sigma^0\pi^0/\Lambda\pi^0$.

We use the values¹⁸

$$\Sigma^-/\Sigma^+ = 2.18, \quad (2.24)$$

$$(\Sigma^- + \Sigma^+)/(\Lambda + \Sigma^0) = 1.8, \quad (2.25)$$

$$0.13 < (\Sigma^- + \Sigma^+ + \Lambda - 2\Sigma^0)/3\Sigma^0 < 0.26. \quad (2.26)$$

These data give the at-rest ratios

$$(\Sigma/\Lambda)_{I=1} \approx 1, \quad (2.27)$$

and

$$\Lambda/(\Lambda + \Sigma^0) \approx 0.2. \quad (2.28)$$

The eight data (2.19)–(2.26) do not warrant the full use of the effective range formalism (2.1)–(2.18) which requires nine “zero-range” $M_{ij}^I(E_0)$ in addition to the ranges R_i . Thus we will introduce the additional assumptions (1) or (2) of Sec. I about the physical nature of the s -wave $\bar{K}N$ reactions which enable us to use the full formalism and will investigate the consequences in Secs. III and IV, respectively.

III. CONSEQUENCES OF ASSOCIATING THE Y_1^* WITH THE $\bar{K}N$ s STATE

The Y_1^* or $\Lambda\pi$ resonance at 1385 Mev has been observed by several experimental groups.³ From study of the angular distribution of the $\Lambda\pi$, there is some indica-

tion that the Y_1^* has a spin $J=\frac{1}{2}$. The position of resonance,

$$1395 \text{ Mev} > E_r > 1375 \text{ Mev}, \quad (3.1)$$

the full width at half maximum,

$$\Gamma_r < 30 \text{ Mev}, \quad (3.2)$$

and ratio of $\Sigma\pi$ to $\Lambda\pi$ associated with the resonance,

$$\alpha(E_r) \equiv \left(\frac{Y_1^* \rightarrow \Sigma\pi}{Y_1^* \rightarrow \Lambda\pi} \right)_{I=1} = 2 \left(\frac{Y_1^* \rightarrow \Sigma^0\pi^-}{Y_1^* \rightarrow \Lambda\pi^-} \right) < 0.2, \quad (3.3)$$

seem fairly well corroborated. Another narrow resonance has recently been observed⁷: the Y_0^* or $I=0$ resonance at ≈ 1405 Mev. Its properties are not at the moment very well determined.

Two years ago, Dalitz and Tuan⁴ analyzed some of the K^-p data in the constant-scattering-length approximation [$a_I(E) = a_I(E_0)$] and found four different types of solutions. One of these solutions has a large positive¹¹ real a_0 [the ($b-$) solution], whereas the ($a-$) solution had a large positive real a_1 . They pointed out the possibility of πV resonances below the K^-p threshold in the $I=0$ or 1 states associated with the ($b-$) or ($a-$) scattering-length solutions, respectively.

Discovery of the Y_1^* led us to discuss⁵ in more detail the hypothesis that the Y_1^* is a quasi-bound state in the s -wave $I=1$ $\bar{K}N$ channel which then decays into the $I=1$ $\Lambda\pi$ and $\Sigma\pi$ channels coupled to it. If we examine the amplitudes $|k\bar{K}^{-1/2}T_{K\Lambda^1}|^2$ and $|k\bar{K}^{-1/2}T_{K\Sigma^1}|^2$ it is easy to see that in the constant-scattering-length approximation that solutions of the ($a-$) type are compatible with the resonance parameters (3.11) and (3.12). On the other hand, it is quite clear that there must be rapid energy dependence present in order to decrease the ratio α from its at-rest value (2.27) to the resonance value (3.3). This fact together with the dependence of the effective range formalism (2.1)–(2.9) on the angular momenta of the $\Lambda\pi$ and $\Sigma\pi$ channels [and thus on the parities $P(K\Lambda N)$ and $P(K\Sigma N)$] provides the impetus for performing a survey of effective range solutions which fit the data (2.19)–(2.26) as well as (3.1)–(3.3). We will only consider the assumption that the Y_1^* is associated with the $\bar{K}N$ s wave, making no assumption whether or not the Y_0^* is. With the *present* above-threshold $\bar{K}N$ data it is not possible to determine whether either resonance must be in this partial wave.

Thus we assume that the Y_1^* has spin $\frac{1}{2}$ and even $P(KY_1^*N)$, and look for effective range solutions which fit the eleven data (2.19)–(2.26) and (3.1)–(3.3). To reduce the number of free parameters, we will assume that there is essentially one range R , i.e., $R_{K^-}^I = R_{\Sigma^I}^I = R_{\Lambda^I}^I \equiv R$. (The derivatives of M_{YY} with respect to k_Y^2 still depend on l_Y .) For each of the four possible combinations of hyperon parities $P(K\Sigma N)$ and $P(K\Lambda N)$, we considered more than 10 000 sets of values for the nine zero-range $M_{ij}^I(E_0)$. Then for each set of $M_{ij}^I(E_0)$,

¹⁶ P. Nordin, University of California Radiation Laboratory Report UCRL-9489, 1960 (unpublished).

¹⁷ Cross sections are measured in mb (1 mb = 10^{-27} cm²).

¹⁸ L. Alvarez, University of California Radiation Laboratory Report UCRL-9354, 1960 (unpublished).

we carried the amplitudes to other energies according to the three different prescriptions: the zero-range approximation $M_{ij}(E) = M_{ij}(E_0)$, $R=0.4$ and $R=0.7$.^{12,19} We emphasize again that our zero-range approximation is *not* equivalent to the constant-scattering-length approximation; for constant M , we see from (2.15) of I that $a(k)$ may still have considerable energy dependence.

The sets of $M_{ij}(E_0)$ were chosen in the following manner: The $\bar{K}N$ scattering lengths evaluated at the K^-p threshold, $a_I(E_0)$, are four input parameters for our computer program. A variety of values are freely chosen subject to the condition that they be of the Dalitz-Tuan ($a-$) type [large positive $\text{Re}a_1(E_0)$] in order to select solutions most likely to lead to the Y_1^* . In addition, all the $a_I(E_0)$ satisfy the at-rest restriction (2.26) on the ratio S of $I=1$ to $I=0$ hyperon production:

$$S(E_0) = \frac{(\Sigma^- + \Sigma^+ + \Lambda - 2\Sigma^0)}{3\Sigma^0} \Big|_{E_0} = \frac{\text{Im}a_1(E_0) |1 - \kappa_{\bar{K}^0}(E_0)a_0(E_0)|^2}{\text{Im}a_0(E_0) |1 - \kappa_{\bar{K}^0}(E_0)a_1(E_0)|^2}. \quad (3.4)$$

The computer then determines the ratio $\alpha(E_0)$ of Σ 's to Λ 's in the $I=1$ state at the K^-p threshold from the measurement (2.25) using the relation

$$\frac{\Sigma^- + \Sigma^+}{\Sigma^0 + \Lambda} = \frac{3S + 2(1 + \alpha)}{(1 + \alpha) + 3\alpha S}. \quad (3.5)$$

The three remaining input quantities are taken to be the $I=1$ K matrix elements (see Sec. II of I) among the hyperon channels: $K_{\Sigma\Sigma^1}(E_0)$, $K_{\Lambda\Lambda^1}(E_0)$, $K_{\Sigma\Lambda^1}(E_0)$. The remaining parameter $K_{\Sigma\Sigma^0}(E_0)$ is then calculated from the Σ^+/Σ^- ratio using the value (2.24). The 9 $M_{ij}^I(E_0)$ are computed from the above set of nine parameters, two of which are measured and seven of which [the $a_I(E_0)$ and three hyperon $K_{YY^1}(E_0)$ matrix elements] are input. There exist two sets of ambiguities (besides the usual ambiguity of π in the phase of the inelastic T -matrix elements) which come from the fact that two of the above quantities (the Σ^+/Σ^- ratio and α) are necessarily positive. Thus for each set of seven input values, four numerically different sets of values of the $M_{ij}(E_0)$ are determined (in addition to the trivial sign differences mentioned above). The range of values used for the input parameters were: $K_{\Sigma\Sigma^1}(E_0)$, seven values ranging from -1.2 to 1.2 ; $K_{\Lambda\Lambda^1}(E_0)$, seven values ranging from -1.1 to 1.1 ; $K_{\Sigma\Lambda^1}(E_0)$, four values ranging from 0.01 to 1.0 (the negative values add nothing new); $a_I(E_0)$, approximately twenty sets of values for the four parameters, $\text{Re}a_0(E_0)$ ranging from -0.4 to 1.0 , $\text{Re}a_1(E_0)$ from 1.00 to 1.25 , $-\text{Im}a_0(E_0)$ from 1.6 to 3.0 , and $-\text{Im}a_1(E_0)$ from 0.14 to 0.25 .

¹⁹ The range R_{K^-} needed to determine the Coulomb corrections [see (2.11)] was, for convenience, taken equal to 0.5 for all the calculations described in this paper.

Thus we start with sets of values for the $M_{ij}(E_0)$ which satisfy the at-rest data (2.24)–(2.26). The computer, using the relations (2.1)–(2.18), determines which of the solutions satisfy the eight other restrictions (2.19)–(2.23) and (3.1)–(3.3). For the “acceptable” effective range solutions, the computer calculates the cross sections (2.14)–(2.18) in the energy range $E_0 < E < 1530$ Mev and the quantities $|k_{\bar{K}^-}^{-1}T_{\bar{K}\Lambda^1}|^2$, $|k_{\bar{K}^-}^{-1}T_{\bar{K}\Sigma^1}|^2$, $|k_{\bar{K}^-}^{-1}T_{\bar{K}\Sigma^0}|^2$ in the energy range $E_0 > E > 1360$ Mev. The calculations required several hours on a CDC 1604 computer.

Only eight acceptable solutions were found. All eight solutions were for the $\Sigma\pi$ channel in a p state, i.e., even $P(K\Sigma N)$ parity [in spite of the fact that approximately twice as many sets of values were investigated for odd $P(K\Sigma N)$ as even]. The number of solutions were evenly divided between even and odd $P(K\Lambda N)$.

In addition, these acceptable solutions all had a range of interaction $R=0.4$ f. The solutions are qualitatively of the quasi-bound state type²: $M_{\bar{K}\bar{K}^1}(E_0)$ is small and negative so that $M_{\bar{K}\bar{K}^1} + K_{\bar{K}}$ vanishes near the position of the Y_1^* . This is the one-channel condition for a bound state. We also note that the $M_{\Sigma\Sigma^I}(E_0)$ were not large so that the combination of a moderately short range, the p -state nature of the $\Sigma\pi$ channel and the values of the $M_{\Sigma\Sigma^I}(E_0)$ led to considerable energy dependence of the $M_{\Sigma\Sigma^I}(E)$ [see (2.7)].²⁰

The acceptable solutions were quite similar in many aspects: (i) The quantity $|k_{\bar{K}^-}^{-1}T_{\bar{K}\Sigma^0}|^2$ fell off very quickly below E_0 ; no resonant behavior, such as seen in $|k_{\bar{K}^-}^{-1}T_{\bar{K}\Lambda^1}|^2$, is found. The possibility that both the Y_1^* and Y_0^* are both associated with the s -wave $\bar{K}N$ system thus seems unlikely. Typical behavior of the hyperon production amplitudes below E_0 is shown in Fig 1(a). (ii) The momentum dependence of $1/a_0$ was very rapid and nonquadratic. On the other hand, $1/a_1$ varied very slowly with energy even though as noted above $M_{\Sigma\Sigma^1}(E)$ was quite energy dependent. (iii) The Σ^-/Σ^+ ratio has its maximum value 2.18 at E_0 . It decreases to ≈ 1 at 175 Mev/c incident K^- laboratory momentum (and then remains fairly constant). The possible extreme rapid variation of Σ^-/Σ^+ indicated by fragmentary experimental results between E_0 and 175 Mev/c (i.e., reaching a value $\gtrsim 5$ at 90 Mev/c) is not found in our solutions. (iv) The solutions all show similar cusp phenomena in the hyperon production cross section at the \bar{K}^0n threshold: $\sigma_{K^-\Sigma^-}$ has a downward step, $\sigma_{K^-\Sigma^+}$ and $\sigma_{K^-\Sigma^0}$ a regular cusp and $\sigma_{K^-\Lambda}$ an inverted cusp. (v) The $\Lambda/(\Lambda + \Sigma^0)$ ratio increases from at rest values ≈ 0.2 to ≈ 0.6 at 300 Mev/c. (vi) The $(\Sigma/\Lambda)_{I=1}$ ratio α which is $\lesssim 0.2$ in the resonance energy and ≈ 1 at E_0 , decreases to a value $\ll 1$ at 300 Mev/c.

²⁰ Another consequence is that if one works back through the uncoupled phase method to determine the K matrix in the πY channels in the absence of coupling to the $\bar{K}N$ channel, the scattering is very large. This is disturbing if we feel that the quasi-bound state should provide a natural picture of the Y_1^* .

A quantitative example of features (iii)–(vi) is shown in Fig. 1(b,c). We note that there is no difficulty in obtaining very small α at the Y_1^* . In the example [Fig. 1(a)] $\alpha \approx 0.05$. On the basis of simple centrifugal barrier arguments⁵ it was not possible to understand such a small α . The charge-exchange cross section does not fall off much from its value of ≈ 12 mb at 175 Mev/ c incident K^- momentum. Even though the statistics on the $\sigma_{K^- \bar{K}^0}$ data are quite poor, this seems to be a disturbing feature of our solutions.

The very strong restriction (2.19) on the elastic cross section was relaxed somewhat in order to test the sensitivity of our results to the actual numerical value. We investigated solutions for which

$$\sigma_{K^- \bar{K}^0}(400 \text{ Mev}/c) < 28. \quad (3.6)$$

While additional effective range solutions were found which were acceptable under the restriction (3.6) but not under (2.19), all these solutions had the same general features mentioned above: $P(K\Sigma N)$ even, $R=0.4$, and (i)–(vii).

IV. GLOBAL SYMMETRY

We will treat, in this section, the compatibility of the hypothesis of global symmetry of the pion baryon interactions with the s -wave K^-p data using the uncoupled phase method formalism presented in Sec. IV of I together with an effective range analysis similar to that described in the previous two sections. (However, we do not require our solutions to fit the Y_1^* resonance.)

Global symmetry gives (neglecting the Σ – Λ mass difference) the following relations between the pion-nucleon K -matrix elements K_{NN}^I and the pion-hyperon K -matrix elements K_{YY}^I which would exist in the absence of influences of the $\bar{K}N$ channel:

$$\begin{aligned} K_{\Sigma\Sigma}^0 &= K_{NN}^{\frac{1}{2}}, \\ K_{\Sigma\Sigma}^1 &= \frac{1}{3}(K_{NN}^{\frac{3}{2}} + 2K_{NN}^{\frac{1}{2}}), \\ K_{\Sigma\Lambda}^1 &= \frac{1}{3}\sqrt{2}(K_{NN}^{\frac{3}{2}} - K_{NN}^{\frac{1}{2}}), \\ K_{\Lambda\Lambda}^1 &= \frac{1}{3}(2K_{NN}^{\frac{3}{2}} + K_{NN}^{\frac{1}{2}}). \end{aligned} \quad (4.1)$$

We will assume that (4.1) describes the uncoupled πY K -matrix elements and that they are related to the actual πY K -matrix elements by (4.10) and (4.11) of I.

For the $I=0$ system we have, from the relations (5.1)–(5.5) of I, for small $k_{\bar{K}}$:

$$K_{\Sigma\Sigma}^0 = \frac{\text{Im}a_0 + (\text{Re}a_0 - R_{\bar{K}})K_{\Sigma\Sigma}^0}{-\text{Im}a_0 K_{\Sigma\Sigma}^0 + \text{Re}a_0 - R_{\bar{K}}}, \quad (4.2)$$

$$(K_{\bar{K}\Sigma}^0)^2 = -k_{\bar{K}} \text{Im}a_0 [1 + (K_{\Sigma\Sigma}^0)^2], \quad (4.3)$$

$$K_{\bar{K}\bar{K}}^0 = -k_{\bar{K}} (\text{Re}a_0 + \text{Im}a_0 K_{\Sigma\Sigma}^0). \quad (4.4)$$

The $I=1$ relations, for the K_{ij} in terms of the uncoupled K^1 , a_1 and α [found using (4.10), (4.11), and (5.5) of I]

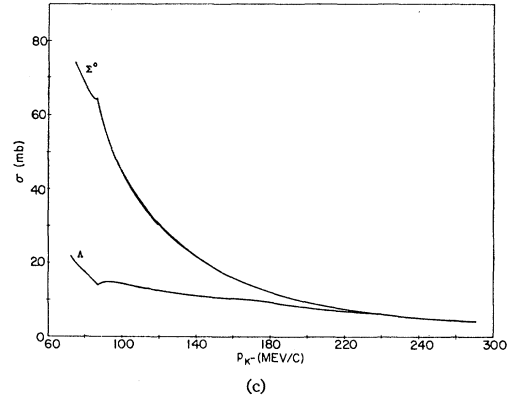
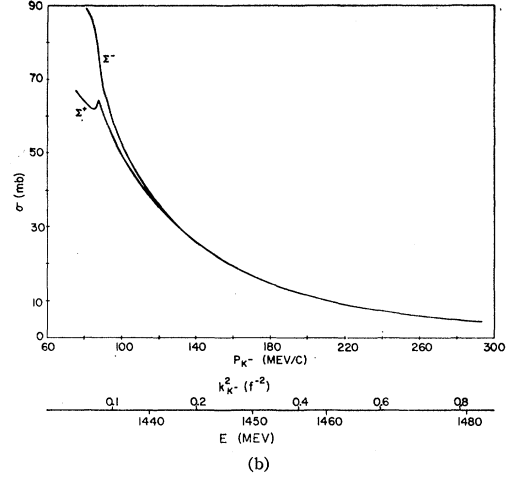
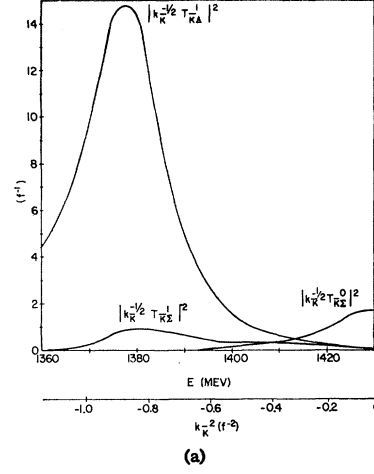


FIG. 1. Example of effective range solution which yields Y_1^* for $l_\Sigma=1$, $l_\Lambda=0$ and $R=0.4$. The zero-range parameters $M_{ij}^I(E_0)$ are $M_{\bar{K}\bar{K}}^0=2.32$, $M_{\Sigma\Sigma}^0=2.73$, $M_{\bar{K}\Sigma}^0=2.65$, $M_{\bar{K}\bar{K}}^1=-0.79$, $M_{\Sigma\Sigma}^1=0.31$, $M_{\Lambda\Lambda}^1=-0.77$, $M_{\bar{K}\Sigma}^1=0.18$, $M_{\bar{K}\Lambda}^1=0.40$, $M_{\Sigma\Lambda}^1=0.51$. (a) The quantities $|k_{\bar{K}}^{-1/2} T_{K\Lambda}^1|^2$ as a function of the total center-of-mass energy E . (b), (c) The cross sections for hyperon production as a function of incident K^- laboratory momentum P_{K^-} .

are more complicated: First we solve the quadratic equation

$$\alpha \equiv |T_{\bar{K}\Sigma}^1/T_{\bar{K}\Lambda}^1|^2 = |x/y|^2,$$

for the quantity

$$\beta \equiv K_{\bar{K}\Lambda^1}/K_{\bar{K}\Sigma^1}, \quad (4.5)$$

where

$$x = 1 + i(\beta \mathbf{K}_{\Sigma\Lambda^1} - \mathbf{K}_{\Lambda\Lambda^1}), \quad (4.6)$$

and

$$y = \beta + i(\mathbf{K}_{\Sigma\Lambda^1} - \beta \mathbf{K}_{\Sigma\Sigma^1}). \quad (4.7)$$

Thus knowing β , x , y , we determine $K_{\bar{K}\bar{K}^1}$ from the relation

$$k_{\bar{K}}^{-1} K_{\bar{K}\bar{K}^1} = -\text{Re} a_1 + \text{Im} a_1 \tan \phi, \quad (4.8)$$

where

$$\begin{aligned} \phi = \text{phase} [1 + (\mathbf{K}_{\Sigma\Lambda^1})^2 - \mathbf{K}_{\Sigma\Sigma^1} \mathbf{K}_{\Lambda\Lambda^1} \\ - i(\mathbf{K}_{\Sigma\Sigma^1} + \mathbf{K}_{\Lambda\Lambda^1})] - \text{phase} (R_{\bar{K}} - a_1) \\ - \text{phase} (x + \beta y). \end{aligned} \quad (4.9)$$

Then introducing

$$\begin{aligned} z = [1 + (\mathbf{K}_{\Sigma\Lambda^1})^2 - \mathbf{K}_{\Sigma\Sigma^1} \mathbf{K}_{\Lambda\Lambda^1} - i(\mathbf{K}_{\Sigma\Sigma^1} + \mathbf{K}_{\Lambda\Lambda^1})] \\ \times (R_{\bar{K}} - a_1)^{-1} (x)^{-1} (k_{\bar{K}}^{-1} \mathbf{K}_{\bar{K}\bar{K}^1} + R_{\bar{K}}), \end{aligned} \quad (4.10)$$

we have

$$k_{\bar{K}}^{-1} (K_{\bar{K}\Sigma^1})^2 = \frac{-\alpha \text{Im} a_1}{(1+\alpha)} |z|^2. \quad (4.11)$$

Finally we solve the pair of equations

$$z = (1 - iK_{\Sigma\Sigma^1}) - iK_{\Sigma\Lambda^1}(y/x), \quad (4.12)$$

$$K_{\Sigma\Lambda^1} = \beta(K_{\Sigma\Sigma^1} - \mathbf{K}_{\Sigma\Sigma^1}) + \mathbf{K}_{\Sigma\Lambda^1}, \quad (4.13)$$

for $K_{\Sigma\Lambda^1}$ and $K_{\Sigma\Sigma^1}$, and determine $K_{\Lambda\Lambda^1}$ from

$$K_{\Lambda\Lambda^1} = \beta^2(\mathbf{K}_{\Sigma\Sigma^1} - K_{\Sigma\Sigma^1}) + \mathbf{K}_{\Lambda\Lambda^1}. \quad (4.14)$$

The uncoupled phase formalism presented above is used to determine the zero-range parameters $M_{ij}(E_0)$ needed for an effective range analysis of the above-threshold s -wave K^-p data (2.19)–(2.26). That is, the relations (4.1)–(4.14) are to be evaluated only at the K^-p threshold, the energy dependence of the cross sections being determined by Eqs. (2.1)–(2.18).

Our procedure to test global symmetry is as follows: Analogous to the method described in Sec. III we choose values of $a_I(E_0)$ satisfying (2.26), which, however, are *not* now restricted to the Dalitz-Tuan ($a-$) type, and determine $\alpha(E_0)$ from (2.25). Then instead of introducing the three $K_{YY^1}(E_0)$ as free parameters, we determine them from the knowledge of the $\mathbf{K}_{YY^1}(E_0)$, $\alpha(E_0)$, $a_1(E_0)$ and a range $R_{\bar{K}}$ using (4.5)–(4.14). The values of πN phase shifts are taken as

$$s_{\frac{1}{2}}: K_{NN^{\frac{1}{2}}}(E_0) = -0.14, \quad K_{NN^{\frac{1}{2}}}(E_0) = 0.22, \quad (4.15)$$

$$p_{\frac{1}{2}}: K_{NN^{\frac{1}{2}}}(E_0) = -0.08, \quad K_{NN^{\frac{1}{2}}}(E_0) = 0.17; \quad (4.16)$$

which yield, from (4.1),

$$P(KYN) \text{ odd: } \mathbf{K}_{\Sigma\Sigma^0}(E_0) = 0.22,$$

$$\begin{aligned} \mathbf{K}_{\Sigma\Sigma^1}(E_0) = 0.10, \quad \mathbf{K}_{\Sigma\Lambda^1}(E_0) = -0.17, \\ \mathbf{K}_{\Lambda\Lambda^1}(E_0) = -0.02; \end{aligned} \quad (4.17)$$

$$P(KYN) \text{ even: } \mathbf{K}_{\Sigma\Sigma^0}(E_0) = 0.17,$$

$$\begin{aligned} \mathbf{K}_{\Sigma\Sigma^1}(E_0) = 0.10, \quad \mathbf{K}_{\Sigma\Lambda^1}(E_0) = -0.12, \\ \mathbf{K}_{\Lambda\Lambda^1}(E_0) = 0.01. \end{aligned} \quad (4.18)$$

The at-rest Σ^+/Σ^- ratio (2.24) then determines $K_{\Sigma\Sigma^0}(E_0)$, which in turn, using (4.2), determines $\mathbf{K}_{\Sigma\Sigma^0}(E_0)$. Thus the at-rest data already provide a test for global symmetry since this $\mathbf{K}_{\Sigma\Sigma^0}(E_0)$ must agree with the value (4.17) or (4.18). We use the criterion that the “calculated” $\mathbf{K}_{\Sigma\Sigma^0}(E_0)$ is “satisfactory” if it satisfies

$$0.0 < \mathbf{K}_{\Sigma\Sigma^0}(E_0) < 0.4. \quad (4.19)$$

If it is satisfactory, we then calculate the $M_{ij}^I(E_0)$.

We note that there are three different types of ranges involved in our calculations: (1) the effective ranges R_i which determine the energy dependence of the $M_{ii}^I(E)$; (2) the range R_{K^-} which determines the Coulomb corrections¹⁹; and (3) the range $R_{\bar{K}}$ which relates the uncoupled $\pi Y K$ matrix elements to the actual ones. We consider two values of $R_{\bar{K}}$ in the uncoupled-phase formalism (4.1)–(4.14):

$$R_{\bar{K}} = 0.5, \quad (4.20)$$

and

$$R_{\bar{K}} = \infty. \quad (4.21)$$

For $R_{\bar{K}} = \infty$, the uncoupled-phase method reduces to the weak coupling approximation for K [see (5.8) of I].²¹

Eighty sets of values for the four input parameters $a_I(E_0)$ were investigated. They were divided up into ranges of values corresponding to the four Dalitz-Tuan types, e.g., the ($b-$) type^{4,11,12} with $\text{Re} a_0$ ranging from 1.6 to 2.3, $\text{Re} a_1$ from -0.3 to 0.5 , $-\text{Im} a_0$ from 0.4 to 3.0 , and $-\text{Im} a_1$ from 0.4 to 0.9 .

Starting with sets of values for the $M_{ij}(E_0)$ which satisfy the at-rest data (2.24)–(2.26) as well as the global symmetry restriction (4.19), the computer, using the relations (2.1)–(2.18) determines which of the solutions satisfy the four above-threshold restrictions (2.20)–(2.23) and the *modified* restriction (3.6) on $\sigma_{K^-K^-}$ (400 Mev/c). As in Sec. III, we used one range R to determine the energy dependence of the $M_{ij}(E)$ according to the three different prescriptions: the zero-range approximation $M_{ij}(E) = M_{ij}(E_0)$, $R = 0.4$ and $R = 0.7$.

The several acceptable effective solutions had the following features: (i) The value range $R_{\bar{K}}$ used in the uncoupled phase procedure was 0.5 in all the acceptable solutions. (ii) Solutions for both even and odd $P(KYN)$ were found. (iii) The solutions had $a_I(E_0)$ of the ($a-$) and ($b-$) type. In fact, the example shown in Fig. 2 yields an $I=0$ resonance similar to the Y_0^* . However, no solution was found which had all the characteristics of the Y_1^* . (iv) One or more of the actual $\pi Y K$ matrix elements $K_{YY^1}^I$ were largely modified from the global-symmetry uncoupled values (4.17), (4.18).

²¹ The relations (4.1)–(4.11) along with (4.21) provided the formalism for computing the K matrices [and thus the $M_{ij}(E_0)$] in Sec. III from the a_I , α , and the $\pi Y K$ -matrix elements $K_{YY^1}^I(E_0)$.

V. DISCUSSION

A. Association of the Y_1^* with the $\bar{K}N$ s State

Since the measurement of $\bar{K}N$ cross sections near threshold are not quite extensive enough at present to permit a meaningful effective range analysis, we have considered two separate assumptions, which, when combined with the $\bar{K}N$ data, do permit this analysis. These two possibilities embody the most natural alternative descriptions of the Y_1^* . The first possibility is that the resonance is to be a quasi-bound state of the $I=1$ s -wave $\bar{K}N$ system.² Assuming that the Y_1^* is in this partial wave, we have made a purely phenomenological analysis of the data. We performed a survey, as distinguished from a search, for solutions. We believe, however, that the qualitative aspects of the acceptable solutions found may characterize any solution. The solutions describe the Y_1^* essentially as a quasi-bound state.^{2,20} The principle qualitative properties are that the $K\Sigma N$ parity is even²² and that there is no room for the Y_0^* resonance⁷ to be associated with the $\bar{K}N$ s state. We have no suggestions to explain the Y_0^* in the framework of this picture of the Y_1^* .

It is of great interest that some experimental results, too vague to be included as conditions in the computing program, are not easy to fit with the solutions found. In particular, $\sigma_{K^- \bar{K}^0}$, as calculated, does not fall off fast at high energies (it is still ≈ 10 mb at the lab momentum $P_{K^-} = 400$ Mev/c) and the $I=1$ Σ/Λ ratio, as calculated, becomes $\ll 1$ for $P_{K^-} \gtrsim 300$ Mev/c, in possible disagreement with experiment. Then there are the results for the Coulomb interference effects in K^-p elastic scattering which we did not make use of. We conclude that with just a little more data, a full search for effective range fits will be justified.

B. Global Symmetry

The second possibility we consider is global symmetry of the "uncoupled" πY phase shifts. In this case the Y_1^* (and the " Y_c^* ," the pion-hyperon resonance recently observed at higher energy,¹⁰ if it turns out to have $I=2$) is presumably analogous to the $p_{\frac{1}{2}}$ πN resonance. Indeed one can bring about a reasonable fit to the Y_1^* measurements²³ (discussed further below). Only a brief survey of effective range fits for the $\bar{K}N$ s states, assuming either even or odd KYN parity, was made. Acceptable solutions were readily found when the restriction (2.19) on $\sigma_{K^- \bar{K}^0}(400 \text{ Mev/c})$ was modified to (3.6).

²² Note added in proof. A $J = \frac{3}{2} \pi Y$ resonance at 1520 Mev has been recently reported: M. Ferro-Luzzi, R. Tripp, and M. Watson, Phys. Rev. Letters 8, 28 (1962); 8, 175 (1962). They conclude from their observations that $P(K\Sigma N)$ is odd, that the resonance corresponds to a d wave for the $\bar{K}N$ channel and that there is very little p wave present at this energy. They find an upper limit on the s -wave elastic K^-p cross section at 400 Mev/c which corresponds to our modified restriction (3.6).

²³ D. Amati, B. Vitale, and A. Stanghellini, Phys. Rev. Letters 5, 520 (1960). T. Lee and C. Yang, Phys. Rev. 122, 1954 (1961).

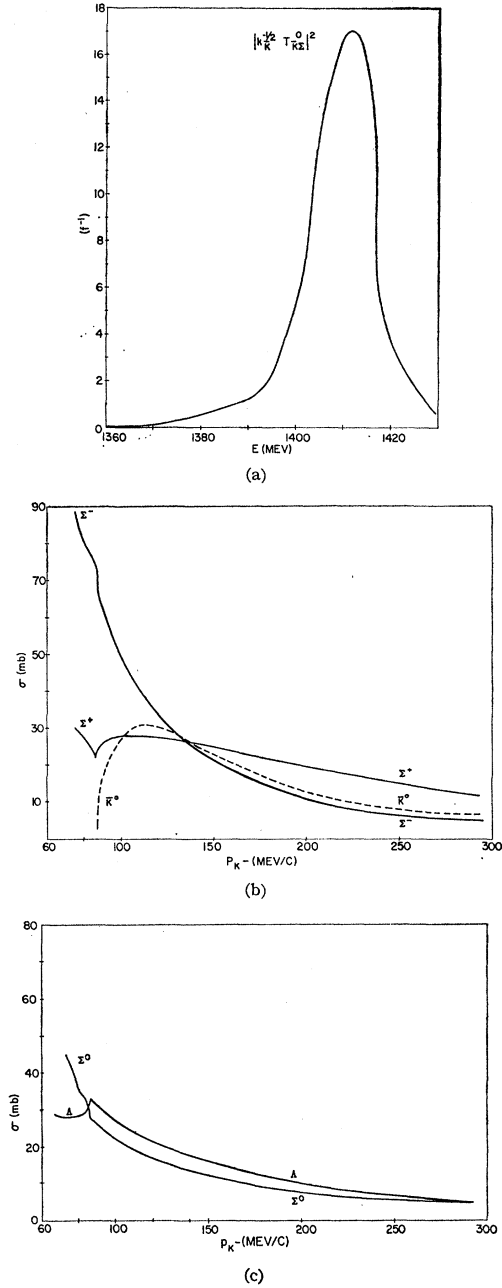


FIG. 2. Example of effective range solution which has uncoupled global-symmetry phases $K_{YY'I}$ for $l_\Sigma = l_\Lambda = 1$. The range $R_{\bar{K}}$ relating the uncoupled to actual phases is 0.5, while the range R determining the energy dependence of the M_{ij} is 0.7. The zero-range $M_{ij}^I(E_0)$ are $M_{\bar{K}\bar{K}^0} = -0.16$, $M_{\Sigma\Sigma^0} = 2.20$, $M_{\bar{K}\Sigma^0} = 0.91$, $M_{\bar{K}\bar{K}^1} = -2.67$, $M_{\Sigma\Sigma^1} = -4.97$, $M_{\Lambda\Lambda^1} = -15.87$, $M_{\bar{K}\Sigma^1} = 1.73$, $M_{\bar{K}\Lambda^1} = -1.08$, $M_{\Sigma\Lambda^1} = -7.85$. (a) The quantity $|k_K^{-1} T_{K\Sigma^0}|^2$ vs E . (The $|k_K^{-1} T_{K\Sigma^1}|^2$ are < 0.2 .) (b), (c) The cross sections for hyperon production and charge-exchange scattering as a function of P_{K^-} .

The results demonstrate again⁹ that the actual πY phases in partial waves coupled to the $\bar{K}N$ s wave are quite different from assumed uncoupled phases. Of course, this does not establish that global symmetry is

not a useful concept for discussing other partial waves or high energies. Recall the criterion (5.8) of **I** which, for example, along with an experimentally-determined scattering length for the $J=\frac{3}{2}$ $\bar{K}N$ channel would enable us to estimate whether a theory which ignores the $\bar{K}N$ channel would give accurate predictions for the Y_1^* and Y_c^* .

We found in our analysis that one can obtain the Y_0^* , i.e., that the $\bar{K}N$ s -wave data and the description of the Y_0^* as a bound $\bar{K}N$ s state is consistent with global symmetry.

Assuming that, consistent with global symmetry, the Y_0^* is a quasi-bound $\bar{K}N$ s state, then we have a picture for both Y_0^* and the Y_1^* and Y_c^* . For completeness, let us examine how the Y_1^* arising from $I=1$ $p_{\frac{1}{2}}$ πY scattering is modified by the $\bar{K}N$ channel. For definiteness consider the latter in a $p_{\frac{1}{2}}$ state, assuming the $d_{\frac{3}{2}}$ yields qualitatively the same results.

From the three-channel effective range expression we find that, for a *narrow resonance*, the full width at half-maximum is

$$\Gamma \approx \frac{2(k_\Lambda^3 + \rho k_\Sigma^3)}{(1+\rho)} (-R_{YY\omega Y} - e R_{\bar{K}\bar{K}\omega\bar{K}})^{-1}, \quad (5.1)$$

where the effective range coefficient for $l=1$ is given in terms of the range of forces R as

$$R_{ii} = -3/R,$$

ω is the reduced energy, ρ is the ratio of the partial width in the Σ channel divided by the partial width in Λ channel omitting kinematical and penetration factors, and e is a positive number which is a function of the M_{ij} 's. For $e \rightarrow \infty$ we have a very narrow resonance associated with a bound $\bar{K}N$ state weakly coupled to the πY channels. For $e \rightarrow 0$ we have the simple πY resonance associated with an attractive πY interaction inside the angular momentum barrier as in global symmetry. The interesting point to note is that the coupling to the $\bar{K}N$ channel must narrow the resonance. In our case $R=\frac{1}{2}m_\pi^{-1}$ from a simple fit to the 3,3 πN resonance, and $\rho=\frac{1}{2}$. For a full width of less than 30 Mev, (5.1) becomes in fermi units

$$\Gamma = 0.44/(1+1.6e) < 0.15,$$

from which $e > 1.2$. Thus a rather strong narrowing is needed from the $\bar{K}N$ channel and we may look in the future to correlating this with $p_{\frac{1}{2}}$ or $d_{\frac{3}{2}}$ $\bar{K}N$ scattering lengths.

At the moment then we can obtain in the above manner a picture for both Y_0^* and the Y_1^* and Y_c^* . A reasonable improvement in the experimental situation will certainly decide whether this rather detailed description is correct.

C. Validity of the Effective Range Approximation

We are interested in discussing the validity of the effective range approximation for describing the $\bar{K}N$

system.²⁴ We need to examine the position of T -matrix singularities (cuts and poles) in physical *and* unphysical sheets which have not been or could not be taken into account in our effective range form. These fall into two groups: (1) those associated with channels which have been neglected, (2) below threshold singularities.

The nearest higher-mass channels one might consider are $Y+2\pi$ and $\bar{K}+N+\pi$. The cross section to the former is very small²⁵ ($\lesssim 2$ mb for center-of-mass energy E up to 200 Mev above the $\bar{K}N$ threshold E_0) so that the weight of its physical cut is small and no resonance in this region could have its mechanism in this channel. The cross section to $\bar{K}+N+\pi$ is negligible below the \bar{K}^*+N threshold²⁵ which is 400 Mev above E_0 . Below E_0 we have a cut in $T_{\bar{K}\bar{K}}$ only, associated with the exchange of two pions between \bar{K} and nucleon, beginning at $E-E_0 \approx -30$ Mev. The effective range form can approximately simulate this with a pole. The only circumstance in which this would not be satisfactory and which would require modification of the formulas used in this work would be the presence of a resonance or very large cross section in $\pi\pi$ scattering very near the $\pi\pi$ threshold (i.e., not the $I=1$ $\pi\pi$ resonance at 750 Mev). Further away, in $T_{\bar{K}Y}$ and $T_{Y\bar{K}}$, there are several poles and relatively short cuts associated with the Λ and Σ states.²⁶ (The nearest one is in the $I=0$ amplitude around 1270 Mev.) Recall that up to n nearby poles are contained in the n -channel effective range form. In order to fit the actual singularities in meaningful detail, and thus bring the coupling constants into the formulas as parameters, expressions with more channels than we used would be needed. Because of these poles, with the number of channels we used, we must recognize that the expressions cannot be accurate far *below* the positions of the Y_1^* and Y_0^* .^{27,28}

D. Conclusion

Aside from the two physical situations we analyzed and which are discussed in (a) and (b) above, we find that it is strongly indicated that with a moderate in-

²⁴ For a general treatment see M. Ross and G. Shaw, Ann. Phys. **13**, 147 (1961).

²⁵ J. Berge, M. Ferro-Luzzi, and A. Rosenfeld (private communication).

²⁶ See M. Nauenberg, Ph.D. thesis, Cornell University, 1960 (unpublished).

²⁷ In πN scattering this is easily done: By considering the two-channel effective range formula one can describe both the nucleon pole and the 3,3 resonance pole (equivalent to the Serber form of the Chew-Low formula) so that the expression is valid over a very wide energy region. In the small-phase-shift states a one-channel expression is adequate.

²⁸ A modification of the 2- and 3-channel effective range expressions used in the present analysis, analogous to the modification of the one-channel effective range expression in πN scattering to include the nucleon pole, is under consideration. The modified theory would yield (in the approximation of large hyperon mass) all the poles associated with the hyperons and perhaps retain sufficient versatility to fit all the data considered here, without an increase in the total number of parameters. See in this connection: K. Wali, T. Fulton, and G. Feldman, Phys. Rev. Letters **6**, 644 (1961).

crease in experimental information a full search for effective range fits to the data for $E \geq E_0$, making no extra assumptions as in this paper, would be practical. We want to discuss this point further.

The very extensive survey of possible solutions which would reproduce the Y_1^* yielded very few solutions. This was true even though, as mentioned in (a) above, several preliminary experimental results were not made use of. Reports of new experimental results²⁹ which we received in course of preparing this manuscript indicate that already much more data, including new types (i.e., separated cross sections on neutral hyperon production), are available and that there are additional events on film which will substantially improve the statistics. These new data can,²⁹ at low energies, still be analyzed with the constant-scattering-length approximation. With better statistics and fitting conditions from higher energy, [such as the condition (2.19) on $\sigma_{K^-K^-(400 \text{ MeV}/c)}$], use of the effective range formalism will be justified. The constant-scattering-length approximation analysis including prediction of hyperon production ratios involves seven real parameters (six "zero-range" parameters and one range for Coulomb effects). The effective range formalism requires just ten (nine zero-range and one range parameter). More than one range parameter could eventually be considered if warranted by the data. Thus the effective range formalism would not be much more difficult for purposes of analysis. It is of course also necessary to repeat the effective range analysis for the different KYN parity cases. The possibility of gaining information concerning the hyperon parities (as in the survey described in Sec. III) adds great interest to this type of analysis.

Further we claim that the constant-scattering-length approximation may not be justified even for energies very close to E_0 . One may look either at the expression (2.15) of **I** for $1/a$ or at the example shown in Fig. 3 to see that the energy dependence of $1/a$ need not be limited to the form or order of magnitude of $\frac{1}{2}Rk\bar{k}^2$ as in the one-channel problem. In Fig. 3 we plot $1/a_0$ vs $k\bar{k}^2$ for typical satisfactory solution that yielded the Y_1^* . The new data²⁹ yields no constant-scattering-length solutions with large real positive¹¹ a and thus in the constant-scattering-length approximation no bound-state type resonance will occur. This result does not rule out the possibility of describing a Y^* as a quasi-bound state for the reason stated above. Indeed, it provides additional interest for an eventual search for effective

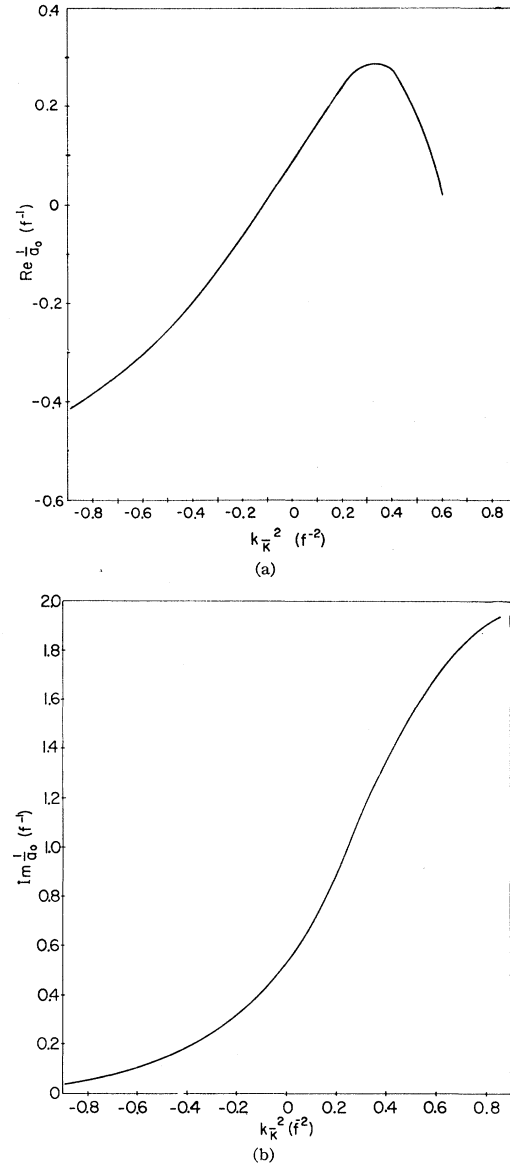


FIG. 3. Variation of $1/a_0$ vs $k\bar{k}^2$ for an effective range solution to the K^-p data which yielded the Y_1^* . The range $R=0.4$ f, $l_2=1$ and $l_A=0$.

range solutions which might accommodate the Y_1^* or Y_0^{*2} .

ACKNOWLEDGMENTS

M.H.R. would like to thank the Instituto de Fisica at University of Rome for its hospitality and the National Science Foundation for a Senior Postdoctoral Fellowship for 1960-1961.

²⁹ W. Humphrey, Ph.D. thesis, University of California Radiation Laboratory Report UCRL-9752, 1961 (unpublished); R. Ross, Ph.D. thesis, University of California Radiation Laboratory Report UCRL-9749, 1961 (unpublished).